

# Firehose constraints for the solar wind suprathermal electrons

M. Lazar,<sup>1,2\*</sup> S.M. Shaaban,<sup>2,3</sup> S. Poedts<sup>2</sup> and Š. Štverák<sup>4,5</sup>

<sup>1</sup> *Institut für Theoretische Physik, Lehrstuhl IV: Weltraum- und Astrophysik, Ruhr-Universität Bochum, D-44780 Bochum, Germany*

<sup>2</sup> *Center for Plasma Astrophysics, KU Leuven, Celestijnenlaan 200B, 3001 Leuven, Belgium*

<sup>3</sup> *Theoretical Physics Research Group, Physics Department, Faculty of Science, Mansoura University, 35516, Egypt*

<sup>4</sup> *Institute of Atmospheric Physics, Czech Academy of Sciences, Prague, Czech Republic*

<sup>5</sup> *Astronomical Institute, Czech Academy of Sciences, Ondřejov, Czech Republic*

Accepted MM DD. Received 2016 MM DD; in original form 2016

## ABSTRACT

The indefinite increase of temperature predicted by the solar wind expansion in the direction parallel to the interplanetary magnetic field is already notorious for not being confirmed by the observations. In hot and dilute plasmas from space particle-particle collisions are not efficient in constraining large deviations from isotropy, but the resulting firehose instability provides in this case plausible limitations for the temperature anisotropy of the thermal (core) populations of both the electron and proton species. The present paper takes into discussion the suprathermal (halo) electrons, which are ubiquitous in the solar wind. Less dense but hotter than the core, suprathermals may be highly anisotropic and susceptible to the firehose instability. The main features of the instability are here derived from a first-order theory for conditions specific to the suprathermal electrons in the solar wind and terrestrial magnetospheres. Unveiled here, new regimes of the electron firehose instability may be exclusively controlled by the suprathermals. The instability is found to be systematically stimulated by the suprathermal electrons, with thresholds that approach the limits of the temperature anisotropy reported by the observations. These results represent new and valuable evidences for the implication of the firehose instability in the relaxation of the temperature anisotropy in space plasmas.

**Key words:** Sun: solar wind — electrons — temperature anisotropy — electromagnetic instabilities — methods: analytical; observational

## 1 INTRODUCTION

In collision-poor plasmas from space large deviations from thermodynamic equilibrium cannot be relaxed by the particle-particle (Coulomb) collisions, but can presumably be constrained by the resulting kinetic instabilities. Thus, if the solar wind expands adiabatically the CGL invariants conserve (Chew et al. 1956) leading to an indefinite increase of temperature in the direction parallel to the interplanetary magnetic field, i.e.,  $T_{\parallel} > T_{\perp}$ . However, the in-situ measurements do not confirm such an increase of their parallel temperature with heliocentric distance, but indicate bounds of the temperature anisotropy of plasma particles (Kasper et al. 2002; Hellinger et al. 2006; Štverák et al. 2008). Because collisions are not efficient, the most invoked mechanism that

can limit the increase of parallel temperature is the firehose instability (Eviatar & Schulz 1970; Kasper et al. 2002; Hellinger et al. 2006; Štverák et al. 2008; Lazar et al. 2014).

The firehose instability driven by the anisotropic electrons with  $A \equiv T_{\perp}/T_{\parallel} < 1$ , also known as the electron firehose instability (EFHI), is particularly important as it can mediate a resonant transfer of (free) energy from electrons to protons (Paesold & Benz 1999; Messmer 2002). This energy transfer from small to large scales is facilitated by the quasi-parallel EFH modes, which are left-handed (LH) circularly polarized and have characteristic frequencies and growth rates in the range of the proton cyclotron frequency. Besides the propagating (non-zero frequency) modes predominant at small angles (quasi-parallel) with respect to the magnetic field direction, the firehose instability may destabilize an additional aperiodic (non-propagating) branch which exists

\* E-mail: mlazar@tp4.rub.de

only for oblique directions (Gary & Nishimura 2003; Camporeale & Burgess 2008; Hellinger et al. 2014). Although it is well known that the suprathermal populations are ubiquitous in the solar wind (Lin 1998; Pierrard & Lazar 2010; Lazar et al. 2012), the anisotropic temperature is in general quantified by a bi-Maxwellian distribution function, which is relevant only for the thermal core of the solar wind electrons. In this case the aperiodic FHI is found to grow faster than the propagating modes, and the instability thresholds approach well enough the limits of the core anisotropy reported by the observations (Štverák et al. 2008). For anisotropies exceeding these thresholds, the free energy is dissipated by the resulting instabilities, which may also scatter particles back towards quasi-equilibrium states and prevent the anisotropy to grow (Gary & Lee 1994; Gary et al. 1998). Instead, for the suprathermal electrons from the solar wind the limits of their anisotropy are markedly departed from the instability thresholds derived for bi-Maxwellian populations, see Figure 6 and the analysis in Štverák et al. (2008). This disagreement may simply be motivated by the fact that suprathermal populations cannot be properly described by the Maxwellian distribution functions, but they can be accurately reproduced by the Kappa power-laws (Vasyliunas 1968; Maksimovic et al. 2005; Pierrard & Lazar 2010). Ubiquitous in the solar wind and subsequent planetary environments, e.g., terrestrial magnetosphere, see the review by Pierrard & Lazar (2010), suprathermal electrons are more dilute but hotter than the core populations. The relaxation through the particle-particle collisions is even less efficient in this case, but kinetic instabilities are expected to explain the limits of temperature anisotropy reported by the observations.

In the present paper we propose a refined analysis of the suprathermal electrons by using a bi-Kappa distribution function to describe the anisotropy of these populations. In the limit of a high power-index  $\kappa \rightarrow \infty$  the (bi-)Kappa distribution function reduces to a (bi-)Maxwellian. Maksimovic et al. (2005) and Štverák et al. (2008) have used the bi-Kappa model to quantify the velocity distributions and the principal properties of the suprathermal electrons in the solar wind, e.g., the components of the anisotropic temperature, parallel ( $T_{\parallel}$ ) and perpendicular ( $T_{\perp}$ ) to the magnetic field direction. The suprathermal electrons are found to be highly anisotropic and with a predominant excess of parallel temperature susceptible to the FHI. The bi-Kappa model was also extensively invoked in theories of dispersion and stability by adopting two alternative assumptions for the temperature of Kappa populations, to be either dependent or independent of the power-index  $\kappa$ . Studies of the FHI (Lazar & Poedts. 2009; Lazar et al. 2011) assume  $\kappa$ -independent temperatures, and find, contrary to the expectations, that the instability is inhibited by the suprathermals and the instability thresholds do not approach but depart even more from the anisotropy bounds of the solar wind suprathermal electrons. However, from a recent analysis on the applicability of Kappa distributions (Lazar et al. 2015, 2016) it becomes evident that a representation with a  $\kappa$ -dependent temperature may provide a more natural interpretation of the suprathermal populations for three fundamental reasons: (1) it corresponds to a Maxwellian limit which reproduces more accurately the thermal (core) population enabling for a direct and realistic comparison (Lazar et al. 2015); (2) the kinetic

instabilities show a systematic stimulation in the presence of suprathermal electrons (Lazar et al. 2015; Viñas et al. 2015; Shaaban et al. 2016a) as one may expect from the excess of free energy accumulated by these populations; and (3) the observations show strong evidence of  $\kappa$ -dependent temperatures, which increase in the presence of suprathermal populations, i.e., temperatures increase with decreasing the power-index  $\kappa$  (Pierrard et al. 2016).

Motivated by these premises, here we re-analyse the instability of the EFH mode by modeling the suprathermal electrons with a bi-Kappa approach with  $\kappa$ -dependent temperatures. In this preliminary analysis we restrict to the same parallel (non-zero frequency) modes studied before by Lazar & Poedts. (2009); Lazar et al. (2011). The bi-Kappa approach is introduced in section 2, enabling us to derive the dispersion relation for the FHI modes. The main features of the instability, are derived and discussed in section 3. In addition, the EFH thresholds are compared with the observations of the suprathermal electron anisotropy. The results of the present work are summarized in section 4.

## 2 BI-KAPPA ELECTRONS. DISPERSION RELATIONS

We first introduce the analytical model for the velocity distributions of suprathermal electrons detected in space plasmas (Maksimovic et al. 2005; Štverák et al. 2008). The suprathermal (halo) electrons are assumed to be a gyrotropic component (isotropic in the plane transverse to the magnetic field) with a bi-axis temperature anisotropy  $T_{\perp} \neq T_{\parallel}$ , where  $\parallel$  and  $\perp$  denote directions relative to the magnetic field. The distribution of suprathermal electrons in velocity space with polar coordinates  $(v_{\perp} \cos \phi, v_{\perp} \sin \phi, v_{\parallel}) = (v_x, v_y, v_z)$  is described by a bi-Kappa distribution function

$$F^{\kappa}(v_{\parallel}, v_{\perp}) = \frac{1}{\pi^{3/2} \theta_{\parallel} \theta_{\perp}^2} \frac{\Gamma[\kappa]}{\kappa^{1/2} \Gamma[\kappa - 1/2]} \times \left( 1 + \frac{v_{\parallel}^2}{\kappa \theta_{\parallel}^2} + \frac{v_{\perp}^2}{\kappa \theta_{\perp}^2} \right)^{-\kappa-1}, \quad (1)$$

which is normalized to unity, and where  $\theta_{\parallel, \perp}$  are thermal velocities defined by, respectively, the parallel and perpendicular temperatures as moments of second order

$$T_{\parallel}^{\kappa} = \frac{m}{k_B} \int dv_{\parallel} v_{\parallel}^2 F^{\kappa}(v_{\parallel}, v_{\perp}) = \frac{\kappa}{\kappa - 3/2} \frac{m \theta_{\parallel}^2}{2k_B}, \quad (2)$$

$$T_{\perp}^{\kappa} = \frac{m}{2k_B} \int dv_{\perp} v_{\perp}^2 F^{\kappa}(v_{\parallel}, v_{\perp}) = \frac{\kappa}{\kappa - 3/2} \frac{m \theta_{\perp}^2}{2k_B}. \quad (3)$$

The bi-Kappa simply reduces to a bi-Maxwellian in the limit of a very large  $\kappa \rightarrow \infty$

$$F^M(v_{\parallel}, v_{\perp}) = \frac{1}{\pi^{3/2} \theta_{\parallel} \theta_{\perp}^2} \exp \left( -\frac{v_{\parallel}^2}{\theta_{\parallel}^2} + \frac{v_{\perp}^2}{\theta_{\perp}^2} \right), \quad (4)$$

with

$$T_{\parallel}^M = \frac{m}{k_B} \int dv_{\parallel} v_{\parallel}^2 F^M(v_{\parallel}, v_{\perp}) = \frac{m \theta_{\parallel}^2}{2k_B} < T_{\parallel}^{\kappa}, \quad (5)$$

$$T_{\perp}^M = \frac{m}{2k_B} \int dv_{\perp} v_{\perp}^2 F^M(v_{\parallel}, v_{\perp}) = \frac{m \theta_{\perp}^2}{2k_B} < T_{\perp}^{\kappa}. \quad (6)$$

Notice in case that the temperature of suprathermal electrons decreases with increasing the power-index  $\kappa$  and reaches a minimum for the Maxwellian limit.

In the direction parallel to the magnetic field ( $\mathbf{k} \parallel \mathbf{B}$ ), the electromagnetic (EM) modes are decoupled from the electrostatic oscillations, and are described by the following general dispersion relation (Gary 1993)

$$\frac{k^2 c^2}{\omega^2} = 1 + \frac{4\pi}{\omega^2} \sum_a \frac{e_a}{m_a} \int_{-\infty}^{\infty} \frac{dv_{\parallel}}{\omega - kv_{\parallel} \pm \Omega_a} \int_0^{\infty} dv_{\perp} \times v_{\perp}^2 \left[ (\omega - kv_{\parallel}) \frac{\partial F_a}{\partial v_{\perp}} + kv_{\perp} \frac{\partial F_a}{\partial v_{\parallel}} \right], \quad (7)$$

where  $\omega$  and  $k$  are respectively, the frequency and the wavenumber of the plasma modes,  $c$  is the speed of light in vacuum,  $\Omega_a = q_a B_0 / (m_a c)$  is the gyrofrequency for the particles of sort  $a$ , e.g.,  $a = e$  for electrons and  $a = p$  for protons, respectively, and " $\pm$ " describes the circularly polarized EM modes with right-hand (RH) and left-hand (LH) polarizations, respectively. For the advanced model introduced in equation (1) the dispersion relation becomes

$$\frac{k^2 c^2}{\omega^2} = 1 + \sum_a \frac{\omega_{a,h}^2}{\omega^2} \left[ A_a - 1 + \frac{(A_a - 1)(\omega \pm \Omega_a) + \omega}{k\theta_{a,\parallel}} Z_{\kappa} \left( \frac{\omega \pm \Omega_a}{k\theta_{a,\parallel}} \right) \right], \quad (8)$$

where  $A_a = T_{a,\perp} / T_{a,\parallel}$  is the temperature anisotropy,

$$Z_{\kappa}(f) = \frac{1}{\pi^{1/2} \kappa^{1/2}} \frac{\Gamma(\kappa)}{\Gamma(\kappa - \frac{1}{2})} \times \int_{-\infty}^{\infty} dx \frac{(1 + x^2/\kappa)^{-\kappa}}{x - f}, \quad \Im(f) > 0 \quad (9)$$

is the Kappa plasma dispersion function (Lazar et al. 2008) of argument

$$f_{\kappa} = \frac{\omega \pm \Omega_a}{k\theta_{a,\parallel}}. \quad (10)$$

In the Maxwellian limit this function reduces to the standard plasma dispersion function (Fried & Conte 1961)

$$Z(f) = \frac{1}{\pi^{1/2}} \int_{-\infty}^{+\infty} dx \frac{\exp(-x^2)}{x - f}, \quad \Im(f) > 0 \quad (11)$$

of argument

$$f = \frac{\omega \pm \Omega_a}{k w_a}. \quad (12)$$

Note that for our model introduced in Eqs. (1)–(6), the anisotropy does not depend on  $\kappa$ , i.e.,  $A = T_{\perp}^{\kappa} / T_{\parallel}^{\kappa} = T_{\perp}^M / T_{\parallel}^M$ .

We investigate the EFHI, which is a LH EM mode driven unstable by an excess of electron temperature in parallel direction  $T_{e,\parallel} > T_{e,\perp}$ , i.e.,  $A_e < 1$ . According to (8), the dispersion relation describing these modes can be rewritten with normalized quantities as follows

$$\mu \left[ A_e - 1 + \frac{A_e(\tilde{\omega} + \mu) - \mu}{\tilde{k} \sqrt{\mu \beta_{e,\parallel}^M}} Z_{\kappa} \left( \frac{\tilde{\omega} + \mu}{\tilde{k} \sqrt{\mu \beta_{e,\parallel}^M}} \right) \right] + \frac{\tilde{\omega}}{\tilde{k} \sqrt{\beta_{e,\parallel}^M / \Theta}} Z \left( \frac{\tilde{\omega} - 1}{\tilde{k} \sqrt{\beta_{e,\parallel}^M / \Theta}} \right) = \tilde{k}^2, \quad (13)$$

where protons are assumed Maxwellian and isotropic  $A_p = 1$ , and  $\tilde{\omega} = \omega / \Omega_p$ ,  $\tilde{k} = kc / \omega_{p,p}$ ,  $\mu = m_p / m_e$  is the proton/electron mass ratio,  $\Theta = T_{e,\parallel}^M / T_{p,\parallel}^M$  is the electron/proton parallel temperature ratio in the Maxwellian limit for both species, and  $\beta_{e,\parallel}^M = 8\pi n_e k_B T_{e,\parallel}^M / B_0^2$  is the parallel electron beta parameter in the Maxwellian limit  $\kappa \rightarrow \infty$ . The dispersion relation for bi-Maxwellian distributed electrons can be obtained from Eq. (13) only by changing  $Z_{\kappa}$  with the Maxwellian plasma dispersion function from (11).

### 3 EFHI. THRESHOLDS VS. SUPRATHERMAL ELECTRON ANISOTROPY

We have solved the dispersion relation (13) numerically, and analyzed the unstable firehose solutions. In this section we present the main features of the EFHI, namely, growth rates, wave-frequencies and wave-numbers, as well as the anisotropy thresholds, and restrict our analysis only to the unstable regimes controlled mainly by the suprathermal electrons. The effects of suprathermal populations are triggered by their temperature anisotropy and their abundance, which is quantified by the finite (especially low) values of the power-index  $\kappa$ .

Firstly, we examine the growth rates and the wave-frequency of the EFH instability for different plasma regimes conditioned in principal by the (parallel) plasma beta parameter,  $\beta_{\parallel}$ , the electron anisotropy  $A$ , and the power-index  $\kappa$ . The regimes identified in Figures 1 and 2 are specific to the firehose instability, when a magnetized plasma becomes penetrable by the LH electromagnetic fluctuations propagating parallel to the magnetic field with frequencies higher than the proton cyclotron frequency. All the unstable modes, i.e., with  $\gamma > 0$  in Figure 1, exhibit this property that becomes evident in Figure 2, where their wave-number dispersion extends to high frequencies exceeding  $\Omega_p$ . In the presence of suprathermals, i.e., at low values of  $\kappa$ , the range of unstable wave-numbers is restrained, but the wave-frequencies and the instability growth-rates are enhanced. These effects are in general stimulated by increasing the plasma beta parameter  $\beta$ , the temperature anisotropy and the electron-proton temperature contrast  $\Theta$ . Plots evidencing the influence of  $\Theta$  are not shown here, but details about this influence are explicitly given in the text. The unstable solutions displayed in Figures 1-4 are obtained for the same value of this parameter, namely, for  $\Theta = 4$  in accordance to the observations in the slow solar wind (Newbury et al. 1998). At higher values of  $\kappa$  the instability conditions may be not satisfied and the electromagnetic modes are damped, e.g.,  $\gamma < 0$  for  $\kappa \geq 6$  in Figure 1, middle and bottom panels. For these modes, the wave-frequency dispersion curves displayed in Figure 2 have a different allure, showing an asymptotic increase similar to the ion (proton) cyclotron modes with frequencies always smaller than  $\Omega_p$ . These are LH modes damped by the protons and therefore limited only to the large (proton) scales. At smaller scales controlled by the electrons (higher wave-numbers) these modes change (mode conversion) to RH polarization (i.e., the wave-frequency displayed in Figure 2 becomes negative) which is more specific to the electron whistlers.

In Figures 3 and 4 we show that these LH-polarized modes with a wave-number dispersion resembling that of the

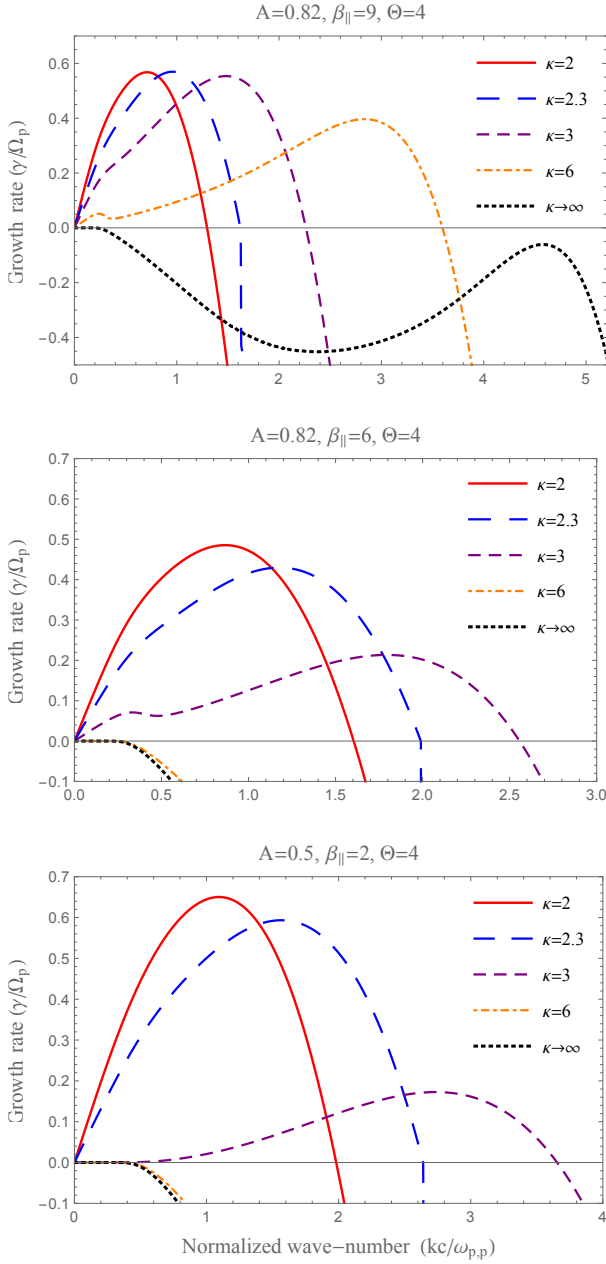


**Figure 1.** Effects of the suprathermal electrons quantified by the power-index  $\kappa = 2, 2.3, 3, 6, \infty$ , on the growth rates of the EFH instability for different plasma beta explicitly given in each panel.

electromagnetic ion cyclotron (EMIC) modes can be destabilized by the anisotropic bi-Kappa distributed electrons, see middle and bottom panels. This is a new regime of the EFHI destabilizing only the low-frequency branch of the LH modes with wave-frequency showing an asymptotic increase of their wave-frequencies but remaining always below  $\Omega_p$ . To establish this regime the kinetic effects of the electrons are also tempered by considering lower values of plasma beta, and the instability is triggered only by the anisotropic distributions with sufficiently low  $\kappa$ , e.g.,  $\kappa < 3$  in Figures 3 and 4. Furthermore, in this case, both the (maximum) growth-rates and the range of the unstable wave-numbers are considerably enhanced by increasing the presence of suprathermals,

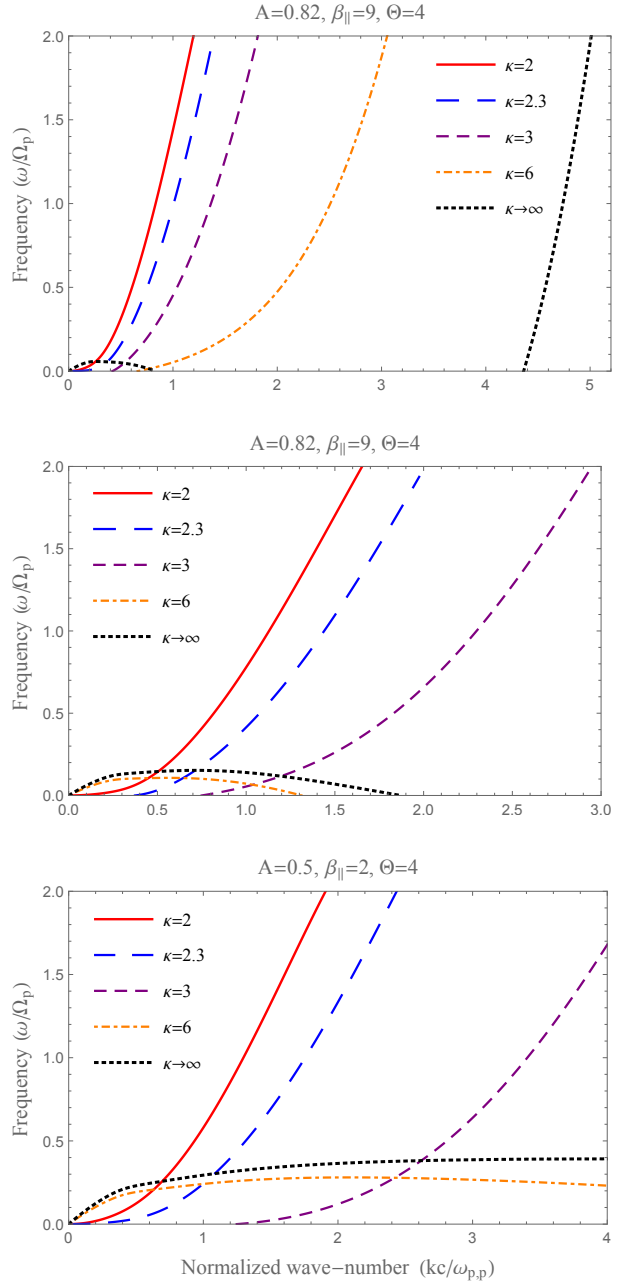


**Figure 2.** Effects of the suprathermal electrons ( $\kappa = 2, 2.3, 3, 6, \infty$ ) on the wave-frequency of the EFH instability for the same cases considered in Fig. 1.

i.e., lowering the values of  $\kappa$ . Again, these features seems to be more specific to the instability of the cyclotron modes Shaaban et al. (2016b). The transition between the classical EFH solutions (exemplified in Figures 1 and 2) and the new regime of a low-frequency EFHI is suggestively shown by the top panels in Figures 3 and 4. In these panels we have unstable solutions specific to both these regimes: the solid-line solution obtained for  $\kappa = 2$  is a classical firehose, while the next long-dashed-line solution obtained for  $\kappa = 2.3$  is already more specific to the new regime of EFHI. In this case it is only the power-index  $\kappa$  that may switch between these two regimes, but a direct comparison of the other plasma parameters in Figures 1-4, clearly shows that these regimes are



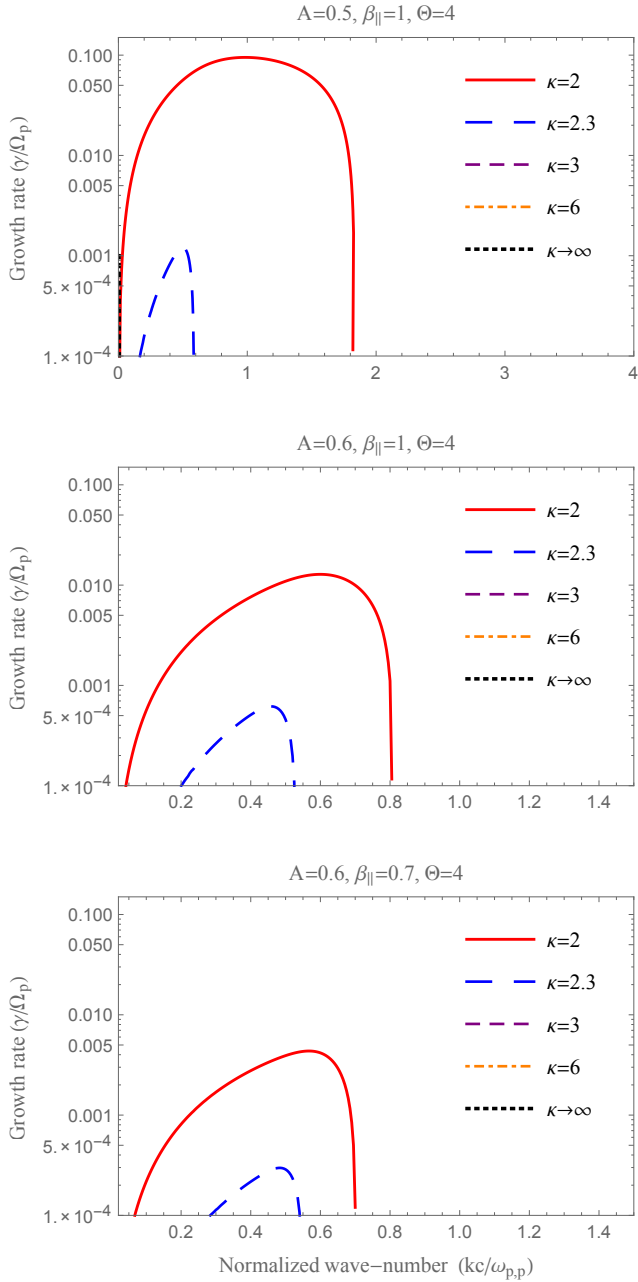


**Figure 3.** Effects of the suprathermal electrons quantified by the power-index  $\kappa = 2, 2.3, 3, 6, \infty$ , on the growth rates of the EFH instability for a lower  $\beta_{\parallel} = 0.6$ .

also conditioned by the temperature anisotropy, the plasma beta, and the temperature contrast between electrons and protons.

In the second part of this section we analyze the anisotropy thresholds of the instability. These thresholds represent plasma conditions associated with given values of the maximum growth-rate, usually small values, e.g.,  $\gamma_m/\Omega_p = 10^{-2}, 10^{-3}$ , approaching the marginal stability  $\gamma_m/\Omega_p \rightarrow 0$ . In Figure 5 we display the instability thresholds associated with  $\gamma_m/\Omega_p = 10^{-3}$  and derived for different values of the electron power-index  $\kappa$ . These are isocontours of the electron temperature anisotropy  $A$  as a function of

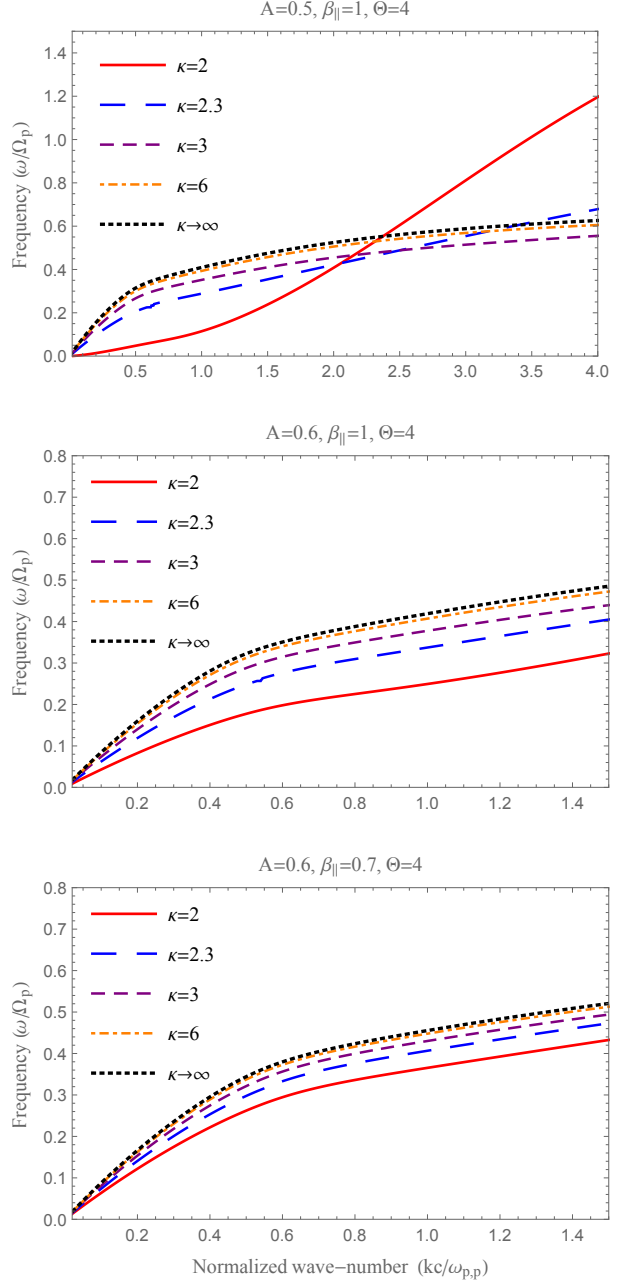


**Figure 4.** Effects of the suprathermal electrons ( $\kappa = 2, 2.3, 3, 6, \infty$ ) on the wave-frequency of the EFH instability for the same cases considered in Fig. 3.

the parallel electron plasma beta  $\beta_{\parallel}$ , fitted to an inverse correlation law of the form (Gary & Lee 1994; Gary et al. 1998)

$$A = 1 + \frac{a}{\beta_{\parallel}^b}. \quad (14)$$

The values obtained for the fitting parameters  $a$  and  $b$  can be found in Table 1. For the plasma beta parameter we consider an extended range of values  $0.1 < \beta_{\parallel} < 50$  relevant for the electron halo populations in the solar wind (Štverák et al. 2008). Higher values of  $\beta_{\parallel}$ , associated with hotter plasmas or less intense magnetic fields, means lower deviations from isotropy to trigger the instability. The effects of

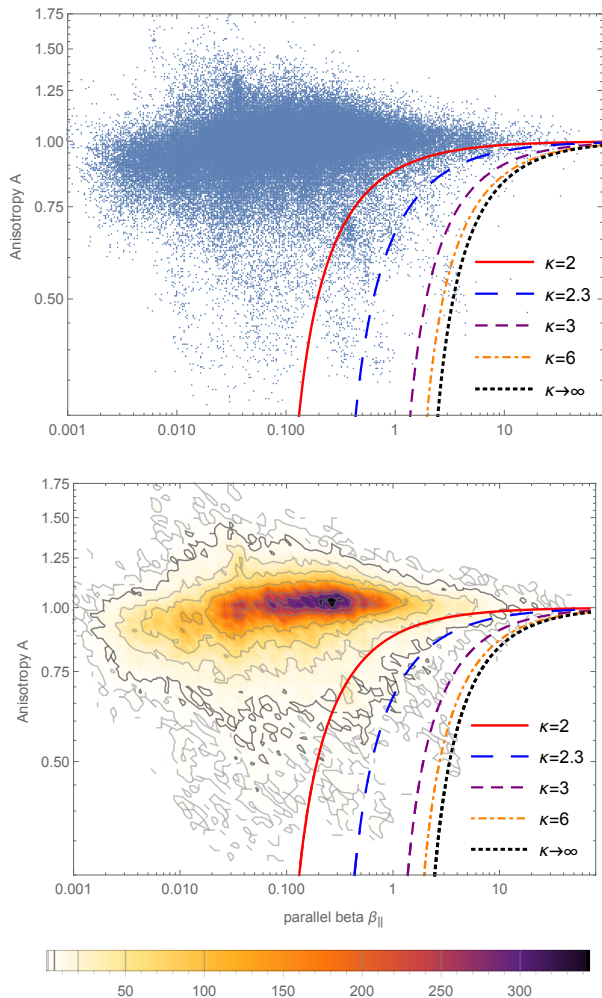


**Figure 5.** Comparison of the anisotropy thresholds (14) for maximum growth rates  $\gamma_m/\Omega_p = 10^{-3}$  with the temperature anisotropy measured in the solar wind which is displayed using a scatter plot data in the top panel and a histogram data in the bottom panel.

suprathermal electrons is reconfirmed here by a systematic stimulation of the (maximum) growth-rates with decreasing  $\kappa$ . As a consequence, the anisotropy thresholds are found to be markedly lowered in the presence of suprathermals, and this effect may be enhanced by increasing the temperature contrast between electrons and protons. Larger variations of the anisotropy thresholds are obtained at lower values of  $\kappa$ .

The instability thresholds are compared in Figure 5 with the observational data of the electron halo populations in the slow solar wind ( $v < 500$  km/s), which are displayed in the top panel as a scatter plot, and in the bottom panel as a histogram counting the number of events within a color logarithmic scale. This data set comprises more than 120 000 events detected by three space missions (Helios 1, Cluster II, and Ulysses) at different heliocentric distances (in the interval 0.3–3.95 AU) in the ecliptic. The details about the electron analyzers used by these missions, and the methods of correction and reconstruction of the 3D velocity distribution functions can be found in Štverák et al. (2008). These authors have used the same set of events to analyze the temper-

**Table 1.** Fitting parameters for thresholds  $\gamma_m/\Omega_p = 10^{-3}$

Fit	$\kappa = 2$	$\kappa = 2.3$	$\kappa = 3$	$\kappa = 6$	$\kappa \rightarrow \infty$
$a$	-0.1196	-0.3304	-0.9615	-1.3733	-1.7950
$b$	0.8708	0.8996	1.0009	1.0030	1.0456

ature anisotropy of the main electron populations, namely, the thermal core and suprathermal halo, and the most plausible constraints exercised on their temperature anisotropy by different physical mechanisms, e.g., collisions and kinetic instabilities. However, Štverák et al. (2008) have limited to investigate in detail only the bi-Maxwellian core anisotropy finding that the particle-particle collisions still may have an effect to constrain low levels of anisotropy, while the kinetic instabilities occur for larger deviations from isotropy, which exceed their thresholds. Indeed, the instability thresholds predicted by a bi-Maxwellian model are found to shape very well the limits of the core anisotropy, but the same thresholds cannot explain the limits observed for the temperature anisotropy of suprathermal electrons. Figure 6 from Štverák et al. (2008) presents such a comparison between the observational data and the EFHI thresholds predicted by a bi-Maxwellian approach, which is also reproduced here in Figure 5 by the dotted line corresponding to  $\kappa \rightarrow \infty$ . Moreover, in Figure 5 we show that this disagreement may be resolved by the instability thresholds derived for bi-Kappa models which are more appropriate to describe the suprathermal electrons. The instability thresholds are markedly changed with decreasing the power index  $\kappa$  and for lower values of  $\kappa$  these thresholds are approaching the limits of the temperature anisotropy observed in the solar wind. What we found even more interesting is that the instability thresholds also shape very well the isocontours of the observational data, counting the number of events in the bottom panel. Developing for large temperature anisotropies exceeding these thresholds, the FHI dissipates the free energy and enhances the electromagnetic fluctuations, which may also prevent the anisotropy to grow by scattering particles back towards quasi-equilibrium states. Given that suprathermal electrons in the solar wind are practically collisionless, such a good agreement between the instability thresholds predicted by the kinetic theory and the limits of the temperature anisotropy reported by the observations represents an important confirmation on the role played by the FHI instability in the relaxation process.

#### 4 DISCUSSIONS AND CONCLUSIONS

In this paper we have proposed a refined theory of the electron firehose instability in anisotropic Kappa distributed plasmas, which provide a new and, in our opinion, valuable evidence of an extended implication of this instability in the relaxation of the temperature anisotropy in collision-poor plasmas from space. Our present study is particularly motivated by the solar wind observations which do not confirm the indefinite increase of temperature predicted by the solar wind expansion in the direction parallel to the interplanetary magnetic field, but reveal very clear bounds for the temperature anisotropy of plasma particles. Previous studies have

focused to the thermal (core) populations of electrons and protons, using standard bi-Maxwellian approaches, and have shown that large deviations from isotropy are constrained by the kinetic instabilities (Hellinger et al. 2006; Štverák et al. 2008). However, the same bi-Maxwellian is not appropriate to describe suprathermal populations and their anisotropy, and cannot prescribe accurately the resulting instabilities and their back reaction on these populations.

Here we have assumed the anisotropic electrons well reproduced by the bi-Kappa distribution function, which is the empirical model invoked by Štverák et al. (2008) to describe the velocity distribution of suprathermal electrons in the solar wind. In addition, the temperature of the suprathermal population is considered dependent on the power-index  $\kappa$ , enabling us a realistic interpretation of the suprathermals and their effects (theoretical and observational arguments are detailed in the Introduction). The results of our present study contrast with those provided by Lazar & Poedts. (2009) and Lazar et al. (2011), who studied the same EFHI but driven by bi-Kappa electrons with a  $\kappa$ -independent temperature. These differences are made clear in the discussion from this section.

Two distinct regimes of the EFHI are identified in Section 3, and these regimes are differentiated by the wave-number dispersion laws (curves) obtained for the wave-frequency and growth-rate of the instability. Thus, more specific to the EFHI are the unstable LH-polarized modes exemplified in Figures 1 and 2 with frequencies that can significantly exceed the proton cyclotron frequency  $\Omega_p$ . For this regime to be established, the kinetic free energy of the anisotropic electrons must be sufficiently large, and this usually means a high enough plasma beta or a large anisotropy. If damped, these modes cannot extend above  $\Omega_p$  and their wave-number dispersion keeps the aspect of low-frequency EMIC modes in the absence of kinetic anisotropies. At higher wave-numbers (lower scales) these damped modes can change their polarity converting to the branch of RH-polarized modes (whistlers). These electromagnetic modes with a wave-number dispersion resembling that of the EMIC modes, i.e., with wave-frequency increasing asymptotically to  $\Omega_p$ , can be driven unstable by the EFHI for conditions approaching marginal stability. A few cases relevant for this new regime are presented in Figures 3 and 4, with mention that top panels include unstable solutions representative for a transition between these two distinct branches of the EFHI.

We should observe that considering plasma parameters with values typical for the solar wind conditions, e.g., in Figures 1-4, the EFHI develops only in the presence of suprathermal electrons, i.e., for finite values of  $\kappa$ , while for (bi-)Maxwellian limit  $\kappa \rightarrow \infty$  these modes are damped. Increasing the presence of suprathermal populations (by lowering  $\kappa$ ) has opposite effects on the wave-frequency of the unstable modes, which become evident if we compare for instance Figures 2 and 4. However, the EFHI is clearly stimulated by the suprathermal electrons, which enhance the (maximum) growth-rates in both these two regimes. Noticeable is the significant increase shown by the growth-rates for conditions approaching the marginal stability (Figure 3), which can also explain the significant decrease of the instability thresholds shown in Figure 5. These thresholds are markedly lowered with decreasing  $\kappa$ , and for lower

values of  $\kappa$  they shape very well the limits of temperature anisotropy reported by the observations in the solar wind. In the previous studies involving bi-Kappa electrons with a  $\kappa$ -independent temperature, e.g., in Lazar & Poedts. (2009); Lazar et al. (2011), the existence of these two distinct regimes was not mentioned, and, in contrast to our present results, the suprathermals were found inhibiting the EFHI, and departing the instability thresholds from the limits of temperature anisotropy in the solar wind.

Our present results strongly suggest that the EFHI may efficiently constrain the temperature anisotropy of the suprathermal electrons in the slow wind, complementing the results by Štverák et al. (2008), which showed the same effects of this instability on the core electrons. A good agreement between the instability thresholds and the bounds of the temperature anisotropy measured in the solar wind is conditioned by a proper modelling of the velocity distributions in accord to the observations. In conclusion, the EFHI can be considered a plausible mechanism of electron energy transfer between the directions parallel and perpendicular to the uniform magnetic field. From an extended perspective, we can further claim that the resulting low-frequency fluctuations can establish an energy transfer from small to large scales, namely from the electrons, especially the energetic or suprathermal electrons which carry the main heat flux in the solar wind, to the resonant protons. Although suprathermal populations are not easily captured in numerical experiments, it becomes however clear that our present results provide valuable premises that may stimulate new and advanced simulations to confirm these mechanisms.

## ACKNOWLEDGMENTS

The authors acknowledge support from the Katholieke Universiteit Leuven, Ruhr-University Bochum, and Alexander von Humboldt Foundation. These results were obtained in the framework of the projects GOA/2015-014 (KU Leuven), G0A2316N (FWO-Vlaanderen), and C 90347 (ESA Prodex 9). The research leading to these results has also received funding from the European Commission's Seventh Framework Programme FP7-PEOPLE- 2010-IRSES-269299 project-SOLSPANET ([www.solspanet.eu](http://www.solspanet.eu)). S.M. Shaaban would like to thank the Egyptian Ministry of Higher Education for supporting his research activities.

## REFERENCES

- Chew G. F. , Goldberger M. L., Low F. E., 1956, Royal Society of London Proceedings Series A, 236, 112
- Camporeale E., Burgess D., 2008, J. Geophys. Res., 113, A07107
- Eviatar A., Schulz, M., 1970, Planet. Space Sci., 18, 321
- Fried B. D., Conte S. D., 1961, The Plasma Dispersion Function. Academic Press, New York
- Gary S.P., 1993, Theory of Space Plasma Microinstabilities, Cambridge University Press, Cambridge.
- Gary S. P., Lee M. A., 1994, J. Geophys. Res., 99, 11297
- Gary S. P., Li H., O'Rourke S., Winske D., 1998, J. Geophys. Res., 103, 14567
- Gary S.P., Nishimura K., 2003, Phys. Plasmas, 10, 3571

- Hellinger, P., Trávníček, P.M., Kasper J.C., Lazarus A.J. 2006, *Geophys. Res. Lett.*, 33, L09101
- Hellinger, P., Trávníček, P.M., Decyk, V.K., Schriver, D. 2014, *J. Geophys. Res.*, 119, 59
- Kasper J.C., Lazarus A.J., Gary S.P., 2002 *Geophys. Res. Lett.*, 29, 1839
- Lazar M., & Poedts S., 2009, *A&A*, 494, 311
- Lazar M., Poedts S., Schlickeiser R. and Ibscher D., 2014 *Sol. Phys.*, 289, 369
- Lazar M., Poedts S., Schlickeiser R., 2011, *A&A*, 534, A116
- Lazar M., Schlickeiser R., Poedts S., 2012, in *Exploring the Solar Wind*, (InTech, Ed. M. Lazar), 241, available from: <http://www.intechopen.com/books/exploring-the-solar-wind/>
- Lazar M., Poedts S., Fichtner H., 2015, *A&A*, 582, A124
- Lazar M., Fichtner H., P.H. Yoon, 2016, *A&A*, in press
- Lazar M., Schlickeiser R., Shukla P. K., 2008, *Phys. Plasmas*, 15, 042103
- Lin R.P., 1998, *Space Sci. Rev.*, 86, 61.
- Messmer, P. 2002, *A&A*, 382, 301
- Maksimovic M., Zouganelis I., Chaufray J.-Y., Issautier K., Scime, E. E., Littleton, J. E., Marsch E., McComas D. J., Salem C., Lin R. P., Elliott H., 2005, *J. Geophys. Res.*, 110, A09104
- Newbury J. A., Russell C. T., Phillips J. L., Gary S. P., 1998, *J. Geophys. Res.*, 103, 9553
- Paesold, G., Benz, A. O. 1999, *A&A*, 351, 741
- Pierrard V., Lazar M., 2010, *Sol. Phys.*, 267, 153
- Pierrard V., Lazar M., Štverák, Š., Poedts S., Maksimovic M., Trávníček P., 2016, *The Electron Temperature Anisotropy in the Solar Wind. I. A comparative analysis of the core and halo populations.* 2016, *Sol. Phys.*(submitted)
- Shaaban S. M., Lazar M., Poedts S., Elhanbaly A., 2016a, arXiv preprint arXiv:1602.04051
- Shaaban S. M., Lazar M., Poedts S., Elhanbaly A., *The interplay of the solar wind proton core and halo populations: EMIC instability*, 2016b, *J. Geophys. Res.*,(submitted)
- Štverák Š., Trávníček P., Maksimovic M., Marsch E., Fazakerley A. N., Scime E. E., 2008, *J. Geophys. Res.*, 113, A03103
- Vasyliunas V. M., 1968, *J. Geophys. Res.*, 73, 2839
- Viñas, A. F., Moya, P. S., Navarro, R. E., Valdivia, J. A., Araneda, J. A., & Muoz, V, 2015, *JGRA*, 120, 3307